DeepWind'2013, 24-25 January, Trondheim, Norway

Use of a wave energy converter as a motion suppression device for floating wind turbines

Michael Borg[a,]*, Maurizio Collu[a], Feargal P. Brennan[a]

aCranfield University, Cranfield, Bedfordshire MK43 0AL, United Kingdom

Abstract

Floating offshore wind turbines (FOWTs) are subjected to large amplitude motions that induce greater loads on components and reduce aerodynamic performance. One approach to counteract this has been to use passive damping systems for FOWTs to dissipate the wave-induced energy and therefore reduce the global platform motions. This paper proposes that rather than discard this energy, a wave energy converter (WEC) is utilized on the floating platform to absorb it. A study is carried out on a floating vertical axis wind turbine (VAWT) combined with WEC moving in heave. A range of damping and stiffness coefficients are applied between the FOWT and WEC to establish strategies for two cases: maximum motion reduction and maximum energy extraction. The results and conclusions obtained are presented in terms of modifying the WEC natural frequency, damping and stiffness values.

Keywords: VAWT; wave energy converter; floating wind turbine; offshore; motion suppression

1. Introduction

As floating offshore wind turbines (FOWTs) become the economically viable option in waters deeper than 50m [1], there is a need to thoroughly understand and model the environment in which they will be operating. In the majority of operational sea states, the FOWTs are subject to significant motions that reduce the aerodynamic performance of the turbine, as well as induce structural loading not encountered with fixed foundations.

One approach to counteract this has been to use passive damping systems for FOWTs to dissipate the wave-induced energy and therefore reduce the global platform motions [2]. This paper proposes that rather than discard this energy, a wave energy converter (WEC) is utilized on the floating platform to absorb it. This would increase the energy yield of the system and actively reduce the global platform motions. Another advantage is that these two energy converters have common infrastructure: a possible

---

* Corresponding author. Tel.: +44 (0)7858 544834.
E-mail address: m.borg@cranfield.ac.uk

combination of the wind and wave energy Power Take-Off (PTO) systems; shared electrical grid connections and shared mooring systems. The progress in identifying optimal damping and stiffness parameters for two cases (maximum energy extraction and motion reduction) is presented in this paper, which is as follows: Section 2 describes the system and sea state under investigation; Sections 3 and 4 describe the methodology and choice of WEC parameters; and Sections 6 and 7 outline the simulations carried out and discuss the results. Finally conclusions about the current work are presented in Section 8.

2. System Description

The floating platform shall be based on the Trifloater semi-submersible presented by Lefebvre and Collu [3], and subsequently fitted with a straight-bladed H-type VAWT presented by Borg et al. [4]. The rotor reaches the rated capacity of 5MW at 15 m/s in a wind profile with vertical power law exponent of 0.11. Table 1 gives the characteristics of the support structure and turbine. The operational site chosen is the Dogger Bank area in the North Sea, which is representative of the environmental conditions present for many offshore wind farms currently being developed. Table 1 also presents the representative JONSWAP wave spectrum parameters [5] that shall be implemented in the time-domain simulations. A water depth of 40 metres shall be assumed.

3. Methodology

Table 1 – Support structure, turbine and JONSWAP spectrum characteristics

In this paper the FOWT investigated is a vertical axis wind turbine (VAWT) mounted on the TriFloater semi-submersible floating platform combined with a hypothetical WEC. This hypothetical WEC was represented by an additional degree of freedom (DOF) in heave. Although one may represent a simple point absorber with damping and stiffness coefficients rather than an extra DOF, this does not seem valid for the problem investigated here. A single-body point absorber needs a reference point which is usually the seabed. In the case of FOWTs, water depth is substantial which would result in unfeasible connections between the PTO and seabed. Another issue is that for a single-body point absorber, efficient energy extraction is obtained when the motion amplitude of the device is large [6], counter to what is trying to be achieved in this study. The FOWT cannot be assumed to be a point absorber and therefore the WEC is being modeled as extra DOFs to be independent of water depth.

Rather than modeling a specific WEC design, trying to optimize it within its dynamic characteristic constraints, here the optimum damping and stiffness

SUPPORT STRUCTURE	
Column radius (m)	5.0
Column height (m)	22.5
Tower-to-column centrelines (m)	30.0
Draught (m)	13.5
Displacement weight (tonne)	3,700.0
Heave natural frequency (rad/s)	0.7345
TURBINE	
Capacity (MW)	5
Rotational speed (rpm)	12
Rated wind speed (m/s)	15
Hub height (m)	72
Radius (m)	37
Blade length (m)	78.75
Blade chord	3.5
Aerofoil section	NACA0018
JONSWAP PARAMETERs	
Significant wave height, H_s (m)	4.928
Philips constant, α	0.008074
JONSWAP constant, β	3.3
Mean zero-crossing period, T_z (s)	10

coefficients were found that would represent the 'ideal' damping device for a given target solution. These optimal coefficients were identified for two cases: maximum motion reduction of the FOWT; and maximum energy extraction by the system. A range of WEC damping values were applied in the numerical model (see Section 4) to understand the effects of the WEC on the motion of the FOWT. In this

work the WEC is considered to have one degree of freedom (DOF), connected to the FOWT heave DOF through a spring-damper coupling.

The motion in heave of semi-submersibles sized for multi-megawatt wind turbines is significant and increases loading on various system components. Therefore it would be beneficial to reduce the platform heave motions to allow for reduced structural loading and hence cheaper capital and operational costs. In fact heave bottom plates have been employed on the WindFloat large-scale prototype installed off Portugal to reduce the platform heave motions [7].

As mentioned before, this is an initial investigation into the effect of a hypothetical WEC on a floating wind turbine. In this study no specific geometrical design of the WEC was set, and hence since the hydrodynamic characteristics are largely dependent on the geometrical shape, they were not considered in the analysis. Whilst the inclusion of the frequency-dependent added mass and damping terms would affect the final results, the above methodology applied here would still be valid once a geometrical WEC design is specified.

4. WEC Parameters

4.1. WEC Inertia

In recent studies of combined wind-wave energy platforms by Peiffer et al. [8] and Muliawan et al. [9], the ratio between the inertia of the WEC and that of the FOWT was found to be close to five percent. For this study three cases shall be investigated. In each case the ratio between the inertia of the WEC and that of the FOWT shall be 2.5 percent (Case 1), 5 percent (Case 2) and 10 percent (Case 3), respectively as shown in Table 2.

Table 2 - WEC parameter values for simulation cases

Case	1	2	3		4
Mass (kg)	9.25×10^4	18.5×10^4	37×10^4	Mass (kg)	18.5×10^4
K_{PTO} (N/m)	4.99×10^4	9.98×10^4	19.95×10^4	B_{PTO} (Ns/m)	4.64×10^4
	ζ	B_{PTO} (Ns/m)	B_{PTO} (Ns/m)	B_{PTO} (Ns/m)	% of ω_n	K_{PTO} (N/m)
A	0.17	2.32×10^4	4.64×10^4	9.28×10^4	25	6.24×10^3
B	0.51	6.96×10^4	13.92×10^4	27.84×10^4	50	24.95×10^3
C	0.85	11.60×10^4	23.20×10^4	46.40×10^4	75	56.14×10^3
D	2.56	34.80×10^4	69.60×10^4	139.20×10^4	150	224.55×10^3
E	7.69	104.40×10^4	208.80×10^4	417.60×10^4	200	399.20×10^3

4.2. WEC Power Take-Off System

The WEC Power Take-Off (PTO) system shall be represented by a linear spring-damper system that is connected to the FOWT in the heave DOF.

4.3. WEC Natural Frequency and Stiffness

Since in this study the only excitation force is being imparted on the WEC by the FOWT, the stiffness of the PTO system shall be set such that the natural frequency of the WEC matches that of the FOWT for Cases 1, 2 and 3 (cf. Table 2). As discussed by literature (e.g. [10]), by matching the natural frequency of the excited body to that of the excitation force, the induced motion shall be greatest. The PTO stiffness, K_{PTO} for each case is given in Table 2.

To investigate the effect of varying the PTO stiffness Case 2A was replicated in Case 4, but in this case the PTO damping was kept constant whilst the PTO stiffness was modified as a percentage of the original WEC natural frequency.

4.4. WEC Power Take-Off Damping

The damping of the PTO system shall be varied for Cases 1, 2 and 3. The values for the PTO damping, B_{PTO}, were chosen to cover a range of damping ratios, ζ. The values for ζ and B_{PTO} for each case are given in Table 2.

5. Numerical Model

5.1. Model Basis

To investigate the dynamics of this system a time-domain model of dynamics was constructed in the MATLAB/Simulink environment using the Marine Systems Simulator Toolbox [11] and an in-house aerodynamic code based on the Double Multiple Streamtube (DMST) model [12] with modifications [13]. The hydrodynamic model is based upon the equation proposed by Cummins [14]:

$$\left(\mathbf{M}_{RB} + \mathbf{A}\right)\ddot{\mathbf{x}}(t) + \int_{-\infty}^{t} \mathbf{K}(t - \tau)\dot{\mathbf{x}}(\tau)d\tau + \overline{\mathbf{C}}\mathbf{x}(t) = \tau_{exc}(t) \qquad (1)$$

Where $\mathbf{M}_{RB}$ is the rigid-body inertia matrix, $\mathbf{A}$ is the infinite-frequency added mass matrix, $\ddot{\mathbf{x}}(t)$ is the body's acceleration, $\mathbf{K}$ is the retardation function matrix, $\dot{\mathbf{x}}(t)$ is the body's velocity, $\overline{\mathbf{C}}$ is the hydrostatic restoring stiffness matrix, $\mathbf{x}(t)$ is the body's displacement, and $\tau_{exc}(t)$ is the wave excitation force and any other external loads, including viscous damping as a fraction of the critical damping.

The coefficients relating to the hydrodynamic added mass, damping and hydrostatic stiffness are obtained from a frequency-domain analysis of the floating platform's geometry. The wave excitation forces as a function of incident wave frequency are also computed in this manner. One issue with Eqn.1 is that the convolution integral representing the radiation forces of the body is computationally inefficient. One approach to solve this is to approximate the convolution integral with a state space model which is inherently computationally efficient as discussed by Taghipour et al. [15] and Borg et al. [16]. The equations of motion now become:

$$\left(\mathbf{M}_{RB} + \overline{\mathbf{A}}\right)\ddot{\mathbf{x}}(t) + \tau_{rad}(t) + \overline{\mathbf{C}}\mathbf{x}(t) = \tau_{exc}(t)$$

$$\dot{\mathbf{z}}(t) = \mathbf{A}'\mathbf{z}(t) + \mathbf{B}'\dot{\mathbf{x}}(t)$$

$$\tau_{rad}(t) = \mathbf{C}'\mathbf{z}(t) + \mathbf{D}'\dot{\mathbf{x}}(t) \qquad (2)$$

Here $z(t)$ and $\dot{z}(t)$ are internal state vectors and the $\mathbf{A}'$, $\mathbf{B}'$, $\mathbf{C}'$ and $\mathbf{D}'$ are constant matrices. The validation of the separate aerodynamic and hydrodynamic models is presented by Collu et al. [17].

Blusseau and Patel [18] found that the gyroscopic forces induced by the coupling between a rotating VAWT and moving platform affect the overall system motions. The gyroscopic forces shall be represented by damping coefficients in pitch and roll. The gyroscopic moments in roll and pitch are given by Equations 3 and 4, respectively:

$$M_{G44} = -I_{zz}\dot{\psi}\dot{\phi} \qquad (3) \qquad\qquad M_{G55} = -I_{zz}\dot{\psi}\dot{\theta} \qquad (4)$$

Where I_{zz} is the moment of inertia of the rotor about its rotational axis, $\dot{\psi}$ is the rotational speed of the rotor which is assumed constant, $\dot{\theta}$ is the angular velocity of the vessel in roll and $\dot{\phi}$ is the angular

$$P_{absorbed} = B_{PTO}\dot{x}_{rel}^{2} \qquad (5)$$

velocity of the vessel in pitch. The DOF of the WEC is included within the equations of motion, resulting in a 7 DOF system. The dynamics model is currently 'semi-coupled', as discussed by Collu et al. [17]. At this point, only the translational and rotational displacements of the floating platform are passed on to the aerodynamic model. In the near future the platform velocities shall be considered within the aerodynamic module. Additionally, the absorbed power of the WEC is calculated using Eq. 5:

6. Numerical Simulations & Results

A total of 20 time-domain simulations were carried out to analyse the case matrix given in Table 2, each with a length of 90 minutes. A total of 1000 harmonic wave components [19] were used to adequately represent the sea spectrum specified in Section 2.

Figs. 1 and 2 present the Response Amplitude Operators (RAOs) for the heave motion of the FOWT and WEC for Case 1, 2 and 3, respectively. A sample time history of the power absorbed by the WEC is shown in Fig. 3, highlighting the variability of power production. Table A.1 in the Appendix presents some statistical data concerning the power absorbed by the WEC, and the heave response of the FOWT and WEC in the operational sea state.

7. Discussion

7.1. WEC Dynamic Response

As expected the peak response of the WEC RAO significantly reduces with increasing damping, as can be seen in Fig. 2. Although the natural frequency of the WEC (assuming a fixed base) was set to 0.7345 rad/s, it can be seen that it has been shifted to lower frequencies due to the interactions with the FOWT. This shift in the peak response of the RAO is greater as the mass of the WEC is increased. On the other hand as the damping is increased, this shift is reduced with more pronounced effects with larger WEC masses. Observing the magnitude of the WEC RAO for Cases 1A, 2A and 3A reveals that at the maximum amplitude, the RAO can be as high as five metres per unit wave height. This is significant and may be impractical in a realistic design, resulting in the use of end-stops to limit the motion of the WEC device. In Case 4, where the PTO stiffness was varied, the peak response of the WEC RAO was significantly reduced when compared to the previous cases. The largest reduction is seen when the PTO stiffness is at its smallest value (Case 4A). This is because lowering the PTO stiffness reduces the transmissibility of the force imparted by the FOWT. This resulted in significantly lower mean WEC amplitudes when the WEC natural frequency was lower than that of the FOWT. This would have positive implications in the detailed design of the WEC, as it can occupy less volume and may undergo lower cyclic loading. In this study any wave forces on the WEC were not considered since they are highly dependent on the geometrical shape of the WEC. The addition of added mass and hydrostatic characteristics would alter the WEC natural frequency. Furthermore the introduction of excitation forces at the incident wave frequency rather than FOWT motion frequency would affect WEC dynamics and so should be considered during future design phases.
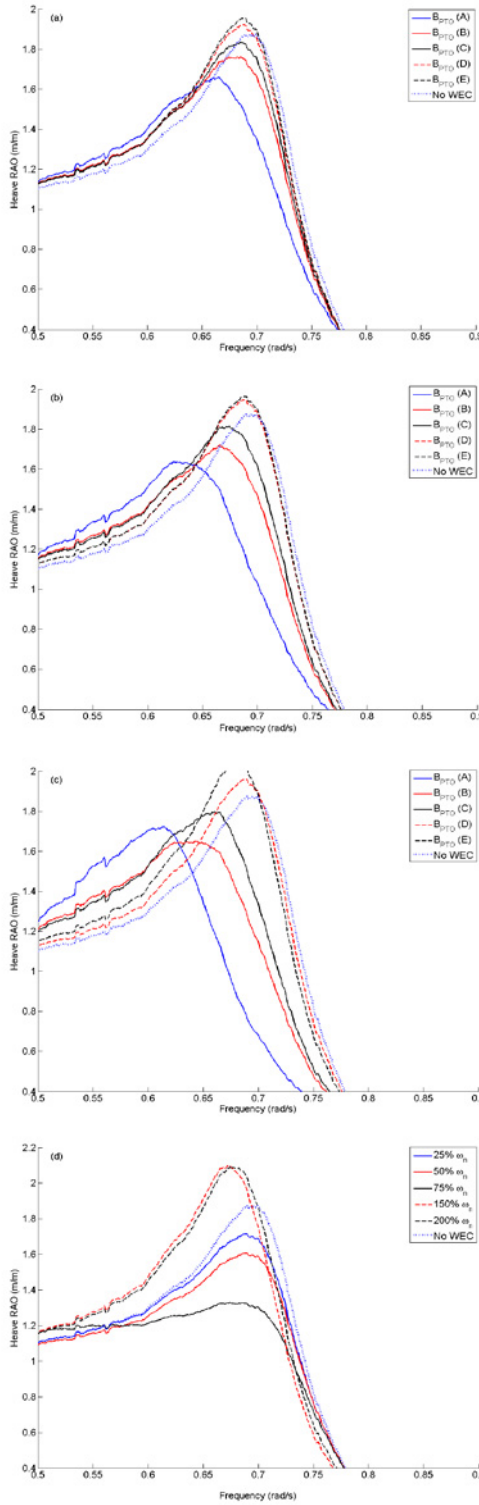
7.2. FOWT Dynamic Response

Figure 1 – FOWT Heave RAO for (a) Case 1;
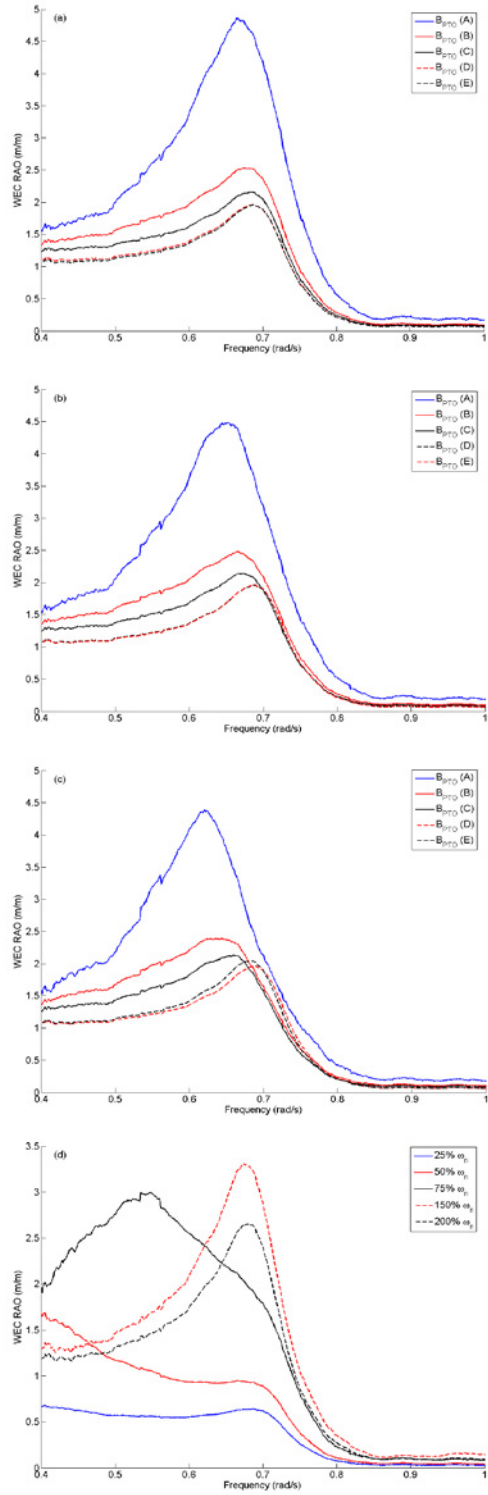(b) Case 2; (c) Case 3; and (d) Case 4

Figure 2 – WEC Heave RAO for (a) Case 1;
(b) Case 2; (c) Case 3; and (d) Case 4

For damping cases A, B and C the peak response of the FOWT heave RAO is reduced, whilst for cases D and E it is increased. This may be due to the fact that for cases A, B and C the damping ratio is below 1, that is, the WEC is an under-damped system. On the contrary for cases D and E the damping ratio is greater that one (over-damped) which would result in a large phase change in the motion of the WEC with respect to the FOWT. This in turn adversely affects the effectiveness of the WEC, such that it is negative.

Whilst there have been positive results regarding modifying the FOWT heave RAO, the operation in the specified sea state has mixed results in Cases 1, 2 and 3. Since the WEC shifted the FOWT heave natural frequency closer to the spectrum peak frequency, the FOWT experiences larger heave motions. Due to the inherent nature of the current connection between the FOWT and the WEC, the natural frequency cannot be shifted to a higher frequency away from the spectrum peak frequency. Only in Cases 1A, 1B and 1C there was a reduction of mean heave amplitude of a few centimeters (cf. Table A.1), which is almost insignificant. Likewise for the other cases, the increase in mean heave amplitude is also almost insignificant.

In Case 4, there is a significantly larger reduction in FOWT heave RAO peak response compared to the previous cases. The greatest reduction was seen when the PTO stiffness was such that the WEC natural frequency was 75 percent of the FOWT natural frequency. When the natural frequency of the WEC was larger than that of the FOWT (Cases 4D, 4E), the WEC had a detrimental effect of the FOWT heave RAO. When operating in the specified sea state, the WEC in Case 4 provided larger reductions in the mean FOWT heave amplitude, although still not greater than 15 percent in Case 4C due to the same reason explained above.
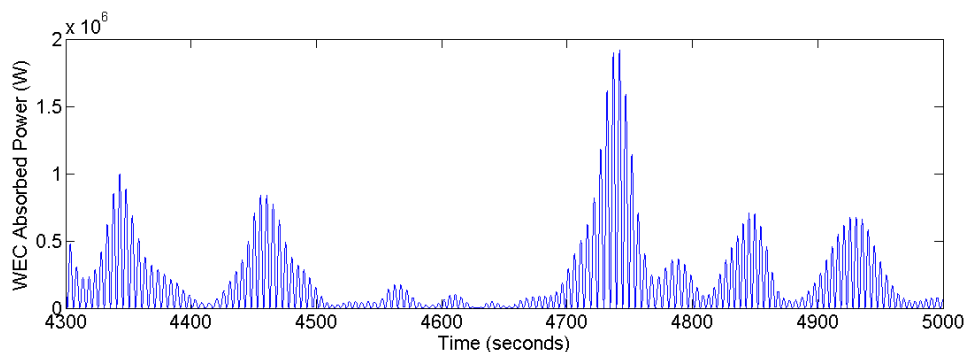

Figure 3 – Sample time history of WEC absorbed power

This effect is very specific to the floating support structure and operational sea state, but it must be noted that the positive effect of the WEC is greatest at the system natural frequency. Through the use of active control systems and more detailed PTO models it may be possible to extend the range of effectiveness of the WEC.

7.3. Power Production

Due to the dependence of the WEC absorbed power on the relative velocity (see Eq. 5), the variation in absorbed power is high. Fig. 3 shows that the absorbed power can vary from zero watts up to almost two megawatts. The variation of the standard deviation of the absorbed power is illustrated in Fig. 4a and Fig. 4b shows the mean absorbed power as a function of WEC mass and damping ratio. It can be seen that while the mean absorbed power is largest at lower damping ratios, the standard deviation is lowest at high damping ratios. This has practical implications on the PTO system: for higher mean absorbed power, the variation in supply is larger, required more robust equipment.

Michael Borg et al. / Energy Procedia 35 (2013) 223 – 233

The mean absorbed power also increases as the mass of the WEC is increased, which is to be expected. As before, the increase in WEC mass also results in higher variations of absorbed power. Both the mean absorbed power and standard deviation appear to decay exponentially with damping ratio, although the current data is limited and so this behavior might be localized. Observing Fig. 4b and Table A.1, it can be seen that the highest absorbed power of almost 138kW is achieved in Case 3A, where the WEC mass is 10 percent of the FOWT mass and the damping ratio is 0.17. Whilst this is approximately 3 percent of the rated capacity of the VAWT, the actual percentage may increase in different met-ocean conditions. In Case 4, the variation of PTO stiffness led to differences in the mean absorbed power and the standard deviation, with increases for both when the WEC natural frequency approached the FOWT natural frequency.

There are number of approaches that may be adopted to increase the absorbed power. Implementing control strategies such as phase control, latching and un-clutching may significantly increase power output and reduce the variability of the absorbed power.
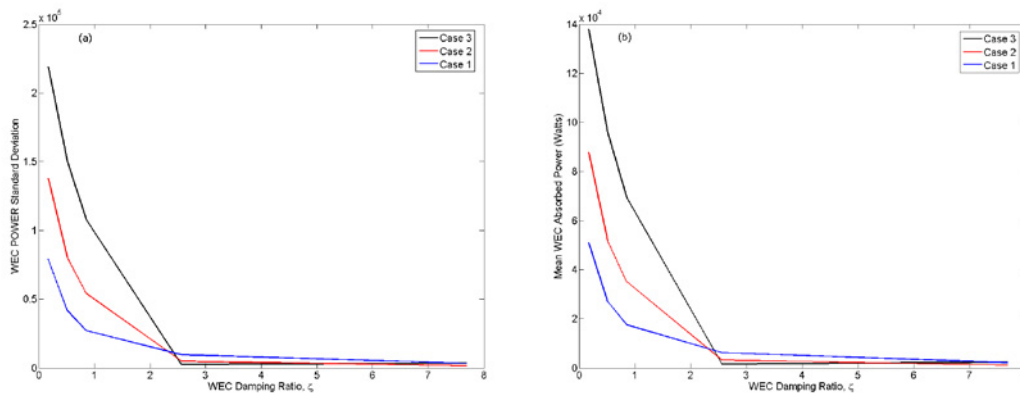

Figure 4 – (a) WEC absorbed power standard deviation as a function of damping ratio; (b) WEC mean absorbed power as a function of damping ratio

7.4. Applicability of Results

Through the above simulations it was found that maximum energy extraction for the specified sea state was obtained in Case 3A, where the WEC mass is 10 percent of the FOWT mass and the damping ratio is 0.17. Case 4 investigated the modification of the PTO stiffness to further reduce the FOWT motion response. It can be seen that there is an inverse relation between mean absorbed power and supply consistency, which will eventually result in a trade-off between these parameters in later stages of design.

Maximum motion reduction was achieved in Case 4C where a reduction of 15 percent of FOWT mean heave amplitude was observed during operation in the specified sea state. The FOWT heave RAO was also reduced by 29 percent.

As can be seen, to achieve the greatest energy extraction, the WEC natural frequency must match the FOWT natural frequency to ensure the greatest induced relative motion between the two bodies. Also the PTO damping should not achieve a damping ratio greater than 1 to allow the WEC to oscillate and produce significant relative motion relative to the FOWT. In this study it was found that the lowest PTO damping produced the most absorbed power. This is most probably due to the relation of power with PTO damping and relative velocity (cf. Eq. 5), as the absorbed power has a squared relation with relative velocity. The low PTO damping required for maximum energy extraction might also lead to reduced systems costs.

On the other hand to achieve maximum FOWT motion reduction, the WEC natural frequency must be shifted to a lower frequency than the FOWT natural frequency. This shift must not be too large, as seen in

Cases 4A and 4B (cf. Table A.1). A shift of 50 percent or more had a smaller effect in motion reduction than a shift of 25 percent (Case 4C). The detriment of shifting the WEC natural frequency is that there is a loss of absorbed power by the WEC, which is more pronounced with larger shifts.

The above characteristics will eventually lead to a trade-off between motion reduction and absorbed power in later stages of design, but it is envisaged that with the appropriate control strategies both of these characteristics may be maximized further. It is important to note that the above results may be localized, that is, since only a range of conditions were investigated it cannot be ensured that these results are the global characteristics.

The results of this study may also be applied to a device that is not a WEC. An internal damping device within the FOWT could be based upon the above PTO system such that excess wave-induced energy is still harvested whilst the device is not subject to the harsh marine environment.

8. Conclusions

This paper introduced the concept of rather than using damping devices to dissipate wave-induced energy from a FOWT, a WEC is implemented to capture this additional energy to increase the system energy yield and make the system more cost effective. An initial numerical study was performed to gain a first insight into the characteristics required of such a WEC, with the following qualitative conclusions:

- Maximum energy extraction from the WEC is achieved by matching the WEC natural frequency to the FOWT natural frequency and using low damping ratios.
- Maximum motion reduction of the FOWT is achieved by shifting the WEC to a lower frequency than the FOWT natural frequency, although this shift must not be too large.

The high variability of the absorbed power at higher values of mean absorbed power is also an issue that may possibly be dealt with through novel control systems and PTO systems. A trade-off between the above two outcomes would be required to ensure the final system is cost-effective.

As noted in Section 3, in this analysis the frequency-dependent added mass and damping of the WEC were not considered. Once the geometrical shape of the WEC is specified, these characteristics will be included in future analyses. It is acknowledged that this inclusion would change the results somewhat, but the methodologies employed and insights gained from this study will still be valid.

This paper has presented the potential of combining wind and wave energy devices to reduce system costs through shared infrastructure, fatigue load reduction and increase the system energy yield. The latter is becoming increasingly important, as the myriad of restrictions of possible ocean energy offshore sites start to limit the available space for arrays of such devices.

Acknowledgements

References

[1]   Jonkman, J. M. and Matha, D. (2011), "Dynamics of offshore floating wind turbines-analysis of three concepts", *Wind Energy,* vol. 14, no. 4, pp. 557-569.

[2]   Roddier, D., Cermelli, C., Aubault, A. and Weinstein, A. (2010), "WindFloat: A floating foundation for offshore wind turbines", *Journal of Renewable and Sustainable Energy,* vol. 2, no. 3.

[3]   Lefebvre, S. and Collu, M. (2012), "Preliminary design of a floating support structure for a 5 MW offshore wind turbine", *Ocean Engineering,* vol. 40, pp. 15-26.

[4]   Borg, M., Utrera Ortigado, E., Collu, M. and Brennan, F. P. (2013), "Passive damping systems for floating vertical axis wind turbines analysis", *European Wind Energy Conference,* 3-7 February, 2013, Vienna, Austria, EWEA, .

[5]   Naess, A. and Moan, T. (2005), "Chapter 5 - Probabilistic Design of Offshore Structures", in Subrata K. Chakrabarti (ed.) *Handbook of Offshore Engineering,* Elsevier, London, pp. 197-277.

[6]   Falnes, J. (2007), "A review of wave-energy extraction", *Marine Structures,* vol. 20, no. 4, pp. 185-201.

[7]   Cermelli, C. A., Roddier, D. G. and Weinstein, A. (2012), "Implementation of a 2MW floating wind turbine prototype offshore Portugal", *Offshore Technology Conference, Proceedings,* Vol. 4, pp. 2678.

[8]   Peiffer, A., Roddier, D. and Aubault, A. (2011), "Design of a point absorber inside the WindFloat structure", *Proceedings of the International Conference on Offshore Mechanics and Arctic Engineering - OMAE,* Vol. 5, pp. 247.

[9]   Muliawan, M. J., Karimirad, M. and Moan, T. (2013), "Dynamic response and power performance of a combined Spar-type floating wind turbine and coaxial floating wave energy converter", *Renewable Energy,* vol. 50, pp. 47-57.

[10]   Falnes, J. (2002), *Ocean waves and oscillating systems: linear interactions including wave-energy extraction,* Cambridge University Press.

[11]   Fossen, T. I. and Perez, T. *, MSS. Marine Systems Simulator (2010)*, available at: http://www.marinecontrol.org (accessed 16.04.2012).

[12]   Paraschiviou, I. (2002), *Wind turbine design: emphasis on the darrieus concept,* 1st ed, Polytechnic International Press, Montreal.

[13]   Shires, A. (2013), "Design optimisation of an offshore vertical axis wind turbine", *Proc. Inst of Civil Engineers, Energy,* vol. 166, no. EN0, pp. 1-12.

[14]   Cummins, W. E. (1962), "The impulse response function and ship motions", *Symposium on Ship Theory,* 25-27 January, 1962, Institut fur Schiffbau, Universitat Hamburg, .

[15]   Taghipour, R., Perez, T. and Moan, T. (2008), "Hybrid frequency-time domain models for dynamic response analysis of marine structures", *Ocean Engineering,* vol. 35, no. 7, pp. 685-705.

[16]   Borg, M., Collu, M. and Brennan, F. P. (2012), "Offshore floating vertical axis wind turbines: advantages, disadvantages, and dynamics modelling state of the art", *The International Conference on Marine & Offshore Renewable Energy (M.O.R.E. 2012),* 26-27 September, 2012, London, RINA, .

[17]   Collu, M., Borg, M., Shires, A. and Brennan, F. P. (2013), "Progress on the development of a coupled model of dynamics for floating offshore vertical axis wind turbines", *Proceedings of the ASME 2013 32nd International Conference on Ocean, Offshore and Arctic Engineering,* 9-14 June, 2013, Nantes, France, ASME, .

[18]   Blusseau, P. and Patel, M. H. (2012), "Gyroscopic effects on a large vertical axis wind turbine mounted on a floating structure", *Renewable Energy,* .

[19]   Faltinsen, O. (1993), *Sea loads on ships and offshore structures,* Cambridge university press.

Appendix A.

Table A.1 - Simulations statistical data

			A	B	C	D	E
Mean Amplitidue	FOWT Heave (metres)	Case 1	0.9031	0.9233	0.9361	0.9535	0.9605
		Case 2	0.8951	0.9247	0.9494	0.9587	0.9623
		Case 3	0.8763	0.9218	0.9688	0.9614	1.0043
		Case 4	0.8875	0.8526	0.7845	1.0306	1.0243
		No WEC	0.9209	0.9209	0.9209	0.9209	0.9209
	WEC Heave (metres)	Case 1	2.3740	1.3269	1.1115	0.9756	0.9628
		Case 2	2.3030	1.3295	1.1280	0.9642	0.9628
		Case 3	2.1762	1.3260	1.1525	0.9626	1.0048
		Case 4	0.3661	0.6092	1.4976	1.5381	1.2615
	WEC Power (kW)	Case 1	50.929	26.847	17.496	6.6258	2.1323
		Case 2	87.947	51.745	35.028	3.1826	1.0708
		Case 3	137.93	95.918	69.49	1.6030	2.3031
		Case 4	24.415	37.329	79.496	9.1410	1.9439
			A	B	C	D	E
Standard Deviation	FOWT Heave (metres)	Case 1	1.1519	1.1785	1.1951	1.2177	1.2267
		Case 2	1.1399	1.1786	1.2103	1.2244	1.2291
		Case 3	1.1162	1.1731	1.2332	1.2279	1.2808
		Case 4	1.1347	1.0903	1.0025	1.3128	1.3045
		No WEC	1.1783	1.1783	1.1783	1.1783	1.1783
	WEC Heave (metres)	Case 1	3.0445	1.6934	1.4182	1.2458	1.2297
		Case 2	2.9484	1.6947	1.4373	1.2313	1.2296
		Case 3	2.7813	1.6880	1.4664	1.2294	1.2813
		Case 4	0.4655	0.7715	1.8984	1.9669	1.6108
	WEC Power (kW)	Case 1	79.222	41.620	27.047	9.6547	3.2823
		Case 2	137.82	80.313	54.060	4.9003	1.6480
		Case 3	218.88	150.22	107.83	2.4673	3.5215
		Case 4	37.716	57.600	125.31	14.014	2.9841
			A	B	C	D	E
Max.	WEC Power (kW)	Case 1	766.65	385.25	246.33	86.578	29.271
		Case 2	1291.4	740.05	493.28	43.774	14.681
		Case 3	2000.8	1345.6	952.13	21.984	31.720
		Case 4	324.97	496.24	1114.0	131.15	28.869